Dual-frequency ultrasound detection of stationary microbubbles in tissue.

B.R. BOLLINGER[1], J.C. WILBUR[2], T.G. DONOGHUE[2], S.D. PHILLIPS[2], D.A. KNAUS[2], P.J. MAGARI[2], D.L. ALVARENGA[3], J.C. BUCKEY[1,3]

[1]*Thayer School of Engineering at Dartmouth College, 8000 Cummings Hall, Hanover, NH 03755;* [2]*Creare, Inc., P.O. Box 71, Hanover, NH 03755;* [3]*Dartmouth Medical School, One Medical Center Dr., Lebanon, NH 03756.*

Bollinger BR, Wilbur JC, Donoghue TG, Phillips SD, Knaus DA, Magari PJ, Alvarenga DL, Buckey JC. Dual-frequency ultrasound detection of stationary microbubbles in tissue. Undersea Hyperb Med 36(2):127-136. Indirect evidence suggests that microbubbles that exist normally in tissue may play a key role in decompression sickness (DCS). Their sizes and locations are unknown. Dual-frequency ultrasound (DFU) exploits bubble resonance to detect bubbles over a wide size range and could potentially detect stationary tissue microbubbles. To test this capability, DFU was used to detect stationary microbubbles of known size (2-3 µm mean diameter) over a range of ultrasound pressures and microbubble concentrations. In gelatin phantoms doped with microbubbles and in *ex vivo* porcine tissue, signals indicative of bubbles were detected for microbubble concentrations of 5×10^5 per mL and greater. Signals were not returned from solid particle microspheres of similar size to the microbubbles or from saline controls. In the thigh of an anesthetized swine, signals were detected for concentrations of 5×10^7 per mL and greater. Because of its ability to detect bubbles over a wide range of sizes, this technique could potentially detect naturally-existing microbubbles in tissue and lead to (a) an improved understanding of the mechanics of bubble formation during decompression and (b) a new metric for evaluating DCS.

INTRODUCTION

With decompression, bubbles may form in the body and can appear in the bloodstream and/or tissue. Decompression sickness (DCS) is a risk to anyone undergoing decompression (moving from a high to low atmospheric pressure), and is a problem of particular interest to the Navy, NASA, and the commercial diving industry. In the 1940's, Harvey (1) demonstrated that bubbles do not arise in isolated blood samples at the levels of decompression that produce bubbles in humans. The conclusion/ hypothesis was that gas nuclei must exist in tissue, and they act as sources for the formation of bubbles when gas diffuses into them during decompression (2). In other words, gas nuclei may exist normally in humans at atmospheric pressure.

DCS risk varies between individuals. Some of the variability may be due to differences in the number and/or size of tissue micronuclei prior to decompression. These micronuclei may be formed by tribonucleation, as muscles shear across one another during physical activity. Several existing models predict bubble growth following decompression assuming the presence of micronuclei (3–6); invasive procedures have directly observed and photographed stationary bubble formation and growth following decompression (7–9), presumably at the sites of pre-existing tissue micronuclei.

To date, no technology has demonstrated the ability to detect pre-existing micronuclei non-invasively. The locations,

sizes, and concentrations of such micronuclei, and the microbubbles that form from them following decompression, remain unknown. Dual-frequency ultrasound (DFU), in which two ultrasound frequencies are transmitted to stimulate bubble responses, may have the capability to detect pre-existing stationary gaseous micronuclei and microbubbles and to monitor changes in tissue microbubble size distributions over time. A technique, such as DFU, that could detect these pre-existing micronuclei and then monitor microbubble growth during and following decompression may be able to provide a better indicator of DCS than conventional bubble detection techniques. Furthermore, these new metrics may be able to be used to study DCS progression, evaluate DCS treatment and mitigation strategies, and provide a better understanding of bubble formation following decompression.

Before using DFU to detect native microbubbles, however, the first step is to insert microbubbles of known size in tissue and to show that detected signals from these bubbles can be distinguished from ultrasonic reflectors of similar size and concentration. While it has previously been shown that DFU can detect large (0.3−1.0 mm) bubbles *in vitro* (10,11), the experimental results presented in this paper are the first demonstration that DFU can be used to detect microbubbles of sizes relevant to the study of DCS *in vivo*.

METHODS

Dual-Frequency Ultrasound

Dual-frequency ultrasound (DFU) is a low mechanical index, nonlinear ultrasound technique that transmits two frequencies instead of one (10). A lower 'pump' frequency, f_p, is used to drive bubbles at their resonant frequency. To detect bubbles of sizes relevant to DCS, the pump frequency can range from the low kHz range to the low MHz range. A second, higher 'image' frequency, f_i, is transmitted as well. When f_i is pulsed, high spatial resolution can be achieved (18). Bubbles of different sizes can be targeted by adjusting the pump frequency. If a bubble of the target size is present in the measurement volume, it will be driven to resonance by the pump frequency. The resulting nonlinear oscillations, under the influence of both f_p and f_i, will cause the bubble to emit the sum, $f_s = f_i + f_p$, and the difference, $f_d = f_i - f_p$, of the two driving frequencies. Detection of sum and difference signals indicates the presence of bubbles of the resonant size.

For detecting decompression-induced microbubbles, DFU has several advantages over nonlinear ultrasound techniques developed for contrast-enhanced sonography. Like other nonlinear techniques, DFU can detect both moving and stationary bubbles, so it can detect both venous gas emboli and stationary microbubbles in tissue. It also has the ability to detect bubbles of many sizes without compromising spatial resolution. In contrast, single frequency harmonic techniques use lower driving frequencies to detect larger microbubbles, which reduces spatial resolution. In DFU, the dedicated broadband pump transducer is used to drive bubbles to resonance over a wide frequency range. So although the pump frequency may be low to detect larger bubbles, the image frequency remains consistently high, resulting in preserved spatial resolution.

For harmonic techniques to detect multiple sizes of bubbles, the transducer needs to transmit over a wide frequency range and detect over an even wider frequency range. With DFU imaging, the image transmit/receive transducer can be more narrowband (therefore less damped and more sensitive) than the transducer for harmonic imaging because the frequency span between f_d and f_s is smaller than the span between f_i and $2f_i$.

It has been previously shown that DFU can detect large (0.4mm and greater) bubbles *in vitro* (10,11), but the ability to detect microbubbles of DCS relevant sizes *in vivo* has not previously been demonstrated. Because the sizes of decompression-induced tissue microbubbles are unknown, the ability to detect bubbles of many sizes without sacrificing sensitivity or resolution will be critical for developing an understanding of tissue bubble formation during DCS.

Device Implementation

The Creare Dual-Frequency Instrument (CDFI) is an evolution of the analog DFU device first implemented by Magari et al (19). Buckey et al (20) have previously demonstrated the ability of the CDFI to detect and characterize bubbles (order 100 µm diameter) transthoracically in the right atrium of an anesthetized swine. The CDFI can be operated in continuous-wave mode (using the technique developed by Newhouse and Shankar (10)) or in pulsed mode (using the technique developed by Cathignol et al (18)). The pulsed mode requires more complicated signal processing, and takes significantly longer to obtain comparable data. Also the high axial resolution provided by pulsed mode was not needed for this study. For these reasons, all of the experiments reported herein were performed using continuous wave ultrasound.

The CDFI uses a National Instruments PXI system and a custom LabVIEW® program to generate signals and perform data acquisition. The experimental setup is shown schematically in Figure 1. Two function generators (NI PXI-5401) produce the two driving signals: pump and image. These signals are each amplified using an RF power amplifier (ENI Model 240L) and sent to the transmitting transducers. The transmit transducers are unfocused, single element PZT piston transducers, the pump transducer having a 2.25 MHz center frequency (Olympus Panametrics-NDT, model V306) and

the image transducer having a 5.0 MHz center frequency (model V309). Each transducer is calibrated, and has a known pressure-voltage relationship in both transmit and receive mode. The receive transducer is a single-element focused transducer (model V382) with a center frequency of 3.5 MHz and a 2.3 cm focal length. The receive signal is amplified (Stanford Research Systems Inc. model SR445A) by a factor of 625, filtered by a bandpass filter around the difference frequency (TTE model KC2-2.75M-10P-50-65A), and sent to a 14-bit, 100 MS/s digitizer (NI PXI-5122) set to a 16.67 MHz sampling rate and a record length of 18205. The digitizer filters the data with a high-frequency, low-pass filter before performing a fast Fourier transform (FFT). To minimize any electrical noise, the digitizer maintains a running average of 50 individual FFTs (Welch's method). This frequency data is then sent to the LabVIEW® program for analysis and display.
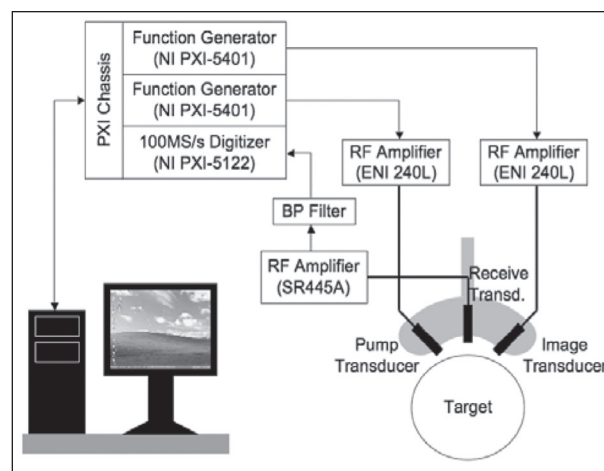

Fig. 1. Schematic of the Creare Dual-Frequency Instrument (CDFI) bubble-detection device.

The transmit and receive transducers are positioned in a custom-made holder such that the axes of all three transducers intersect at 2.5cm from the face of each transducer. The holder-unit is handheld against the subject in a manner similar to a clinical ultrasound

probe. This allows for flexible positioning of the transmit and receive transducers while maintaining the necessary alignment.

Bubble Model and Controls

To demonstrate the ability, and to quantify the sensitivity, of DFU to detect stationary microbubbles transcutaneously *in vivo*, microbubbles of known size and in known concentrations were needed. This was accomplished by using known concentrations of microbubbles from a commercial ultrasound contrast agent (UCA) (Definity®, Bristol-Meyers Squibb Medical Imaging, North Billerica, MA). These microbubbles have a mean diameter of 2−3 μm and consist of C_3F_8 gas stabilized by a lipid shell. While resonance frequency depends on microbubble size, shell material, and thickness (21), these UCA microbubbles are comparable in resonance frequency to the smallest microbubbles that are hypothesized to form during decompression, and so are a good choice for this application.

Solutions of solid polymer microspheres (polylactic acid particle standard, 2 μm diameter, 1% solid, Postnova Analytics, Salt Lake City, UT) were used as a control, as were injections of pure saline. The solid polymer microspheres (SPM) have roughly the same size distribution as the UCA microbubbles, but are solid particles, and thus non-resonant at the frequencies used here.

Experiments were performed using UCA microbubble and SPM solutions with concentrations ranging from 10^5/mL to 10^{10}/mL. All dilutions were made using sterile saline.

Experimental Protocols

In vitro Protocol: Gelatin phantoms were created with three layers. The initial layer was pure gelatin. The second layer was the doped gelatin, made by mixing appropriate quantities of microbubble or SPM solutions with warm, colored gelatin immediately prior to the solidification of the gelatin. This created a center gelatin layer with known concentrations of embedded microbubbles. The third and final layer was again pure gelatin. Multiple phantoms were made, each with a different known concentration of microbubbles or SPM. The phantoms were placed in a water tank and imaged with the CDFI along the length of the phantom. An ultrasonic damping tile (Aptflex F28, Precision Acoustics, Dorset, UK) was used to reduce reflections in the tank. Ultrasound at the image and pump frequencies were transmitted at several pressures, and multiple measurements at each transmit pressure were taken.

Ex vitro Protocol: Known concentrations of microbubbles were injected into swine tissue (pork loin). The transducers were coupled to the tissue with ultrasound gel. Multiple measurements at several transmit pressures were made at baseline and following each injection.

In vivo Protocol: Three swine weighing approximately 20 kg each were anesthetized initially using 20 mg/kg ketamine and 0.05 mg/kg xylazine by intramuscular injection. After initial anesthesia, the swine were kept on approximately 1 L/min O_2 with 2% isoflurane for the duration of the experiments. Atropine (0.04 mg/kg) was given to reduce secretions. A 5x5 grid with 2.5 cm spacings was drawn on the thigh, and grid points were chosen as measurement locations based on their physical properties (i.e. fleshy, joint, etc.). Only fleshy sites were used for this experiment. Each potential measurement site was scanned using clinical 2-D ultrasound to insure that no bones or major vessels were in the measurement volume.

Multiple measurements at several transmit pressures were made prior to injection of the solution. The solution (0.5cc) was then injected transcutaneously at the measurement site at a depth of 2.5 cm. Following injection

of the solution, multiple measurements were taken at each transmit pressure. This process was repeated for each solution at a different injection site. Solutions were injected in the order in which they were least likely to influence subsequent measurements (via diffusion/ perfusion), based on their nonlinear properties: saline first, followed by the lowest to highest concentrations of SPM, followed by the lowest to highest concentrations of microbubbles.

The research protocol followed guidelines set forth by the Dartmouth Institutional Animal Care and Use Committee and was approved by the committee.

Statistical Analysis

Ten to 15 successive measurements were taken at each sample/location both with and without bubbles present. A single-tailed, two-sample T-test assuming unequal variances was used to determine whether the mean of the difference signal detected from samples/ locations with microbubbles was equal to the mean of the difference signal detected from samples/locations without microbubbles.

RESULTS

Initial validation and optimization experiments

Initial validation experiments were performed *in vivo* using 0.5cc injections of microbubbles (undiluted, at 1.2×10^{10}/mL) in the thigh of a swine. Significant mixing signals were detected following injection of the microbubbles, indicating that the CDFI could detect stationary microbubbles *in vivo* (Figure 2). These initial experiments were used to determine the optimum pump and image frequencies for subsequent experiments. While the relationship between resonance frequency and bubble diameter is known, the resonance is broad for 2−3 μm diameter bubbles, and

other factors such as the microbubble shell, frequency-dependent tissue attenuation, and transducer sensitivities affect the selection of pump and image frequencies. To increase sensitivity, pump and image frequencies were chosen to produce a difference signal close to the center frequency of the receive transducer. Image and pump frequencies of f_i = 5.0 MHz and f_p = 2.25 MHz respectively, with a receive transducer with center frequency f_r = 3.5 MHz, yielded the maximum difference signal response from injected microbubbles.
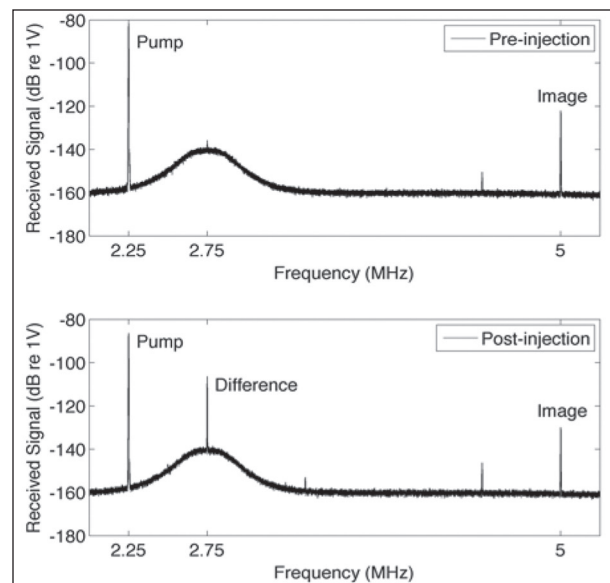

Fig. 2. Dual-frequency ultrasound data of a target area in the hip of an anesthetized swine before and after injection of microbubbles. The bulge in the noise floor is due to the receive bandpass filter at 2.75MHz. Reflected signals at the image and pump frequencies are detected in both cases. ABOVE: Prior to injection of the microbubbles, only small difference signal at 2.75 MHz is detected in the target area (due to tissue nonlinearities). BELOW: Following injection of the microbubbles, significant difference signal at 2.75 MHz is seen.

Effect of transmit pressure

Gelatin and gelatin doped with microbubbles (10^8/mL) were interrogated with DFU at multiple transmit pressures, ranging from 178 dB re 1μPa (768 Pa peak) to 198 dB re 1μPa (7680 Pa peak). The emitted difference

signal is shown in Figure 3. At each transmit pressure, the difference signal detected from the microbubble-doped portion of the gelatin phantom was greater than the difference signal detected from the portion of the gelatin phantom without microbubbles (P < 0.001). As transmit pressure was increased, the difference signal emitted by resonating microbubbles increased linearly. Solid particles (SPM) did not emit significant difference signal, regardless of transmit pressure.
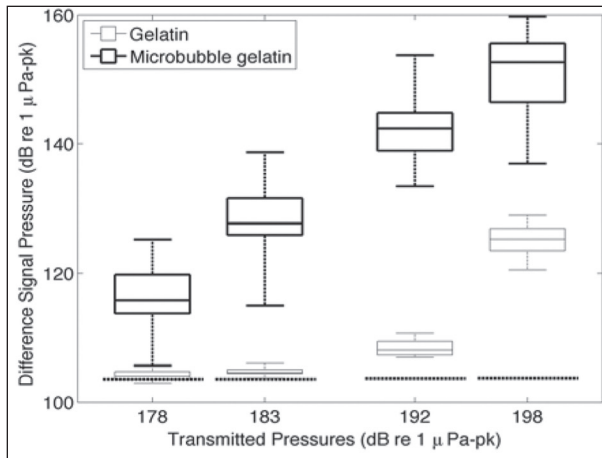

Fig. 3. Difference signal detected from gelatin and gelatin with microbubbles (10^8/mL). At each transmit pressure, the difference signal detected for microbubble gelatin is greater than that detected for plain gelatin (P < 0.001). Each box indicates the median and upper and lower quartiles. The whiskers indicate the maximum and minimum points. The heavy dashed line segments indicate the sensitivity threshold of the device.

The difference signals detected from plain gelatin at the two highest transmit pressures (192 and 198 dB re 1 μPa_{peak}) are significantly greater than the sensitivity threshold of the device (P < 0.001). This is due to reflections within the testing tank and nonlinear co-propagation of the pump and image signals. For test phantoms containing microbubble concentrations of 5×10^5/mL and below, the acoustic damping tile was used in the tank to reduce these effects (as shown in Figure 5).

The effect of transmit pressure was investigated *in vivo* as well, as shown in Figure 4. Difference signal was measured at each site prior to and following injection of the microbubbles. At transmit pressures of 183, 192, and 198 dB re 1 μPa_{peak}, the difference signal detected following injection of the microbubbles was greater than that detected prior to injection (P < 0.001).

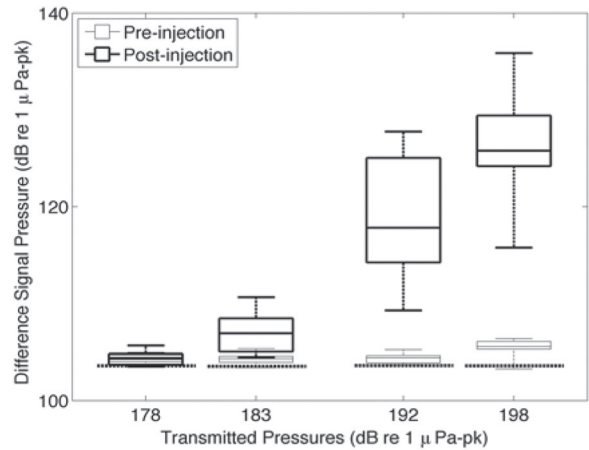**Fig. 4.** Difference signal detected prior to and following injection of microbubbles (10^8/mL) in vivo. At a transmit pressure of 183 dB and above, the difference signal detected following injection is greater than that detected prior to injection (P < 0.001). Each box indicates the median and upper and lower quartiles. The whiskers indicate the maximum and minimum points. The dashed line indicates the sensitivity threshold of the device.

Effect of microbubble concentration

As previously noted, the presence of pre-existing gaseous micronuclei is speculative, as is the size and concentration of microbubbles that grow from them. Because there is such uncertainty regarding tissue bubble populations, theoretical models of bubble formation in tissue have had to consider concentrations ranging from 10^0/mL to 10^{10}/mL (22). In this study, concentrations of microbubbles ranging from 10^5/mL to 1.2×10^{10}/mL were probed with DFU *in vitro*, *ex-vivo*, and *in vivo* using pump and image transmit pressures ranging up to 198 dB re 1 μPa_{peak}.

The difference signals detected from microbubble-doped (various concentrations) and non-microbubble sections of gelatin

phantoms are shown in Figure 5. At concentrations of 5×10^5/mL and above, the difference signal detected from gelatin with microbubbles was significantly greater than the signal detected from plain gelatin (P < 0.001). The difference signal detected from the plain gelatin is above the sensitivity threshold of the device (especially for the measurements of the 10^6, 10^7, and 10^8/mL phantoms, for which the acoustic damping tile was not used in the experimental setup). This base level of detected difference signal can be attributed to the nonlinear co-propagation of the pump and image signals.
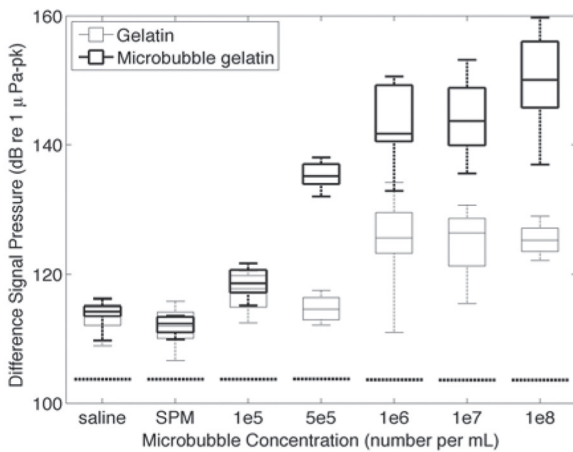
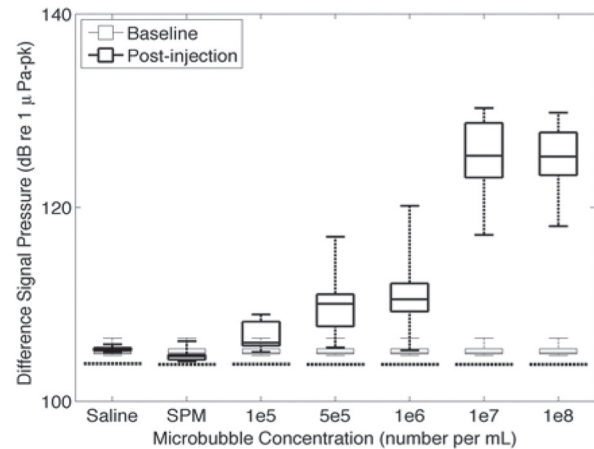do not adversely influence the detected signal amplitudes.

Fig. 6. Ex-vivo concentration results: difference signal detected prior to and following injection of microbubbles. The signal post-injection is greater than the signal prior to injection at concentrations of 5×10^5/mL and above (P < 0.001). Each box indicates the median and upper and lower quartiles. The whiskers indicate the maximum and minimum points. The dashed line indicates the sensitivity threshold of the device.

Fig. 5. In vitro concentration results: difference signal detected from gelatin and gelatin with varying concentrations of microbubbles. At concentrations of 5×10^5/mL and above, the signal from microbubble-doped gelatin is greater than the signal from pure gelatin (P < 0.001). Each box indicates the median and upper and lower quartiles. The whiskers indicate the maximum and minimum points. The dashed line indicates the sensitivity threshold of the device

The same detection threshold was found in *ex-vivo* studies (Figure 6). The detected difference signal at locations of injected microbubbles was greater than the difference signal at baseline for injected microbubble concentrations of 5×10^5/mL and above (P < 0.001). The similarity of the *in vitro* and *ex-vivo* concentration sensitivity thresholds indicates that the differences in coupling and attenuation

Initial measurements *in vivo* indicated that the difference signal detected following injection of microbubbles could be transient in some cases. In some of these cases, clinical 2D ultrasound indicated the presence of blood vessels. Since the purpose of the study is to use injected microbubbles to model the microbubbles that may form in tissue due to decompression, injection sites without ultrasonically detectable blood vessels were chosen. Detected difference signals prior to and following injection of microbubbles *in vivo* is shown in Figure 7. A different site was used for each solution injection. Signals were not transient in the time scale of the measurements (minutes). Difference signal detected following injection of microbubbles was greater than signal detected prior to injection for concentrations of 5×10^7/mL and above (P < 0.001).
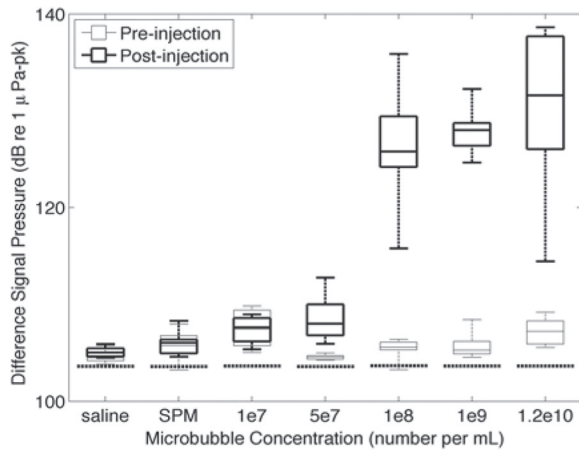
Fig. 7. In vivo concentration results: difference signal detected prior to and following injection of microbubbles. The signal post-injection is greater than the signal prior to injection at concentrations of 5×10^7/mL and above (P < 0.001). Each box indicates the median and upper and lower quartiles. The whiskers indicate the maximum and minimum points. The dashed line indicates the sensitivity threshold of the device.

DISCUSSION

These studies demonstrate that microbubbles can be detected with DFU at a concentration of 5×10^5/mL and above in gelatin phantoms and *ex-vivo* tissue, and at 5×10^7/mL and above in *in vivo* tissue. Solid particle microspheres and injected saline did not return signals. Higher difference signals were returned at higher ultrasonic pressures, with non-linear signals occurring at baseline at ultrasonic pressures of 192dB and above, indicating that sources of non-linearity not related to injected bubbles exist in tissue. The increase in signal seen after inclusion of bubbles in the measurement volume is due to the nonlinear response of the bubbles to DFU.

Effect of increasing ultrasonic pressure

The results showed that the difference signal detected from bubbles in gelatin or bubbles in tissue increased with increasing ultrasonic pressures, but increasing ultrasonic pressure also led to difference signals at baseline. Bubbles, when driven to resonate under dual-frequency excitation, emit signals at the sum and difference of the driving frequencies. Detection of these mixing signals indicates bubbles of the resonant size. However, other sources of nonlinearity, both physical and equipment related, also have the potential to emit mixing signals when driven bi-harmonically.

Two potential equipment-related sources of nonlinearities (and hence false positives) are (a) the electronics of the bubble detection device and (b) the transducers themselves. Benchtop studies in the laboratory investigating detected fundamental and harmonic signals have shown that both of these potential sources of nonlinearity are insignificant and that the difference signals detected in the gelatin and tissue studies are not from either the electronics or the transducers.

Besides the presence of bubbles, nonlinear propagation of ultrasound through the phantom and tissue is another physical source of nonlinearity that can create small amplitude mixing signals. The effect is manifested in figures 3 to 7 by the difference signal amplitude measured at baseline. In the tissue samples and in the swine, signals produced by this effect were just above the sensitivity threshold of the device. *In vitro*, they were more pronounced, most likely due to the significantly lower ultrasonic attenuation of water compared to tissue. This allows for multiple reflections and longer propagation path lengths within the experimental setup.

Since the amplitudes of difference signals produced by both oscillating bubbles and by nonlinear propagation are linearly related to the pressure of the driving signals (10,23), an increase in the transmit pressures will increase the signal detected both with bubbles and at baseline. This is evident in figures 3 and 4. As the pump and image transmit pressures

increase, the difference signal detected from bubbles increases as well. However, the difference signal detected at baseline also increases. Therefore, once transmit pressures are high enough for difference signal to be detected above the noise floor at baseline, no further increase in sensitivity can be achieved by increasing transmit pressures.

Device sensitivity

The data in figures 5 to 7 indicate that the difference signal emitted by bubbles decreases with decreasing bubble concentration. Therefore, sensitivity to bubble concentration is limited by the point at which the signal from bubbles is comparable to the signal produced by tissue nonlinearities. This study indicates that the 2−3 μm diameter microbubbles used in this study are detectable *in vitro* and *ex vivo* at injected concentrations of 5×10^5/mL and above, and *in vivo* at injected concentrations of 5×10^7/mL and above. As a comparison, the concentration of red blood cells in the blood is 5×10^9/ml (24). The microbubble concentrations cited here are injected microbubble concentrations. The actual concentration of the microbubbles *in vivo* may be lower due to dispersion and diffusion of the microbubble solution during and after injection.

DFU to detect decompression-induced microbubbles

Bubbles that form due to decompression can range in size from submicrometer to millimeter in scale (from pre-existing gas nuclei to the large VGE observed with 2D ultrasound). To detect bubbles ultrasonically by exploiting their nonlinear behavior, they must be driven near their resonance. Small bubbles (1−20 μm diameter) exhibit broad frequency responses, especially when stabilized by an encapsulating shell (21). Larger bubbles exhibit much narrower frequency responses and resonate at much lower frequencies. In this study, 2−3 μm

diameter bubbles were used because of their availability and ease of use in creating solutions of known size and concentration. This allowed for the validation of the ability of DFU to detect stationary bubbles in tissue.

By using a broadband transducer to transmit a variety of different pump frequencies, DFU could probe for bubbles of multiple different sizes over a wide size range. The pressure sensitivity of the device, determined by the receive transducer, is not affected. By scanning through pump frequencies, histograms of bubbles sizes present can be created. The ability to detect bubbles of multiple sizes without compromise is the principal advantage of DFU. This ability may allow for DCS symptoms to be correlated with the presence of bubbles of various sizes.

CONCLUSIONS

Dual-frequency ultrasound has the ability to detect bubbles of all sizes without compromising sensitivity or spatial resolution. To the authors' knowledge, this is the first demonstration that DFU can detect stationary microbubbles in tissue. Concentrations of microbubbles as low as 5×10^5/ml were detected *in vitro*, and as low as 5×10^7/mL (0.06% free gas phase by vol.) were detected *in vivo*. This technology can be applied to detect bubble formation in tissue during activity and decompression. The ability to detect bubble formation in tissue following different decompression protocols would be useful in testing bubble growth models, assessing DCS risk, and eventually could lead to a new understanding of the mechanics of bubble formation during decompression and DCS.

REFERENCES

1. Harvey EN. Physical factors in bubble formation. In: Decompression Sickness, Fulton JF, eds. W. B. Saunders Company Ltd, 1951.
2. Hempleman HV. History of decompression procedures. In: by Bennett PB, Elliot DH, eds. The Physiology and Medicine of Diving. WB Saunders, 1993.
3. Van Liew HD, Hlastala MP. Influence of bubble size and blood perfusion on absorption of gas bubbles in tissue. *Respir. Physiol* 1969; 7: 111–121.
4. Van Liew HD. Simulation of the dynamics of decompression sickness bubbles and the generation of new bubbles. *Undersea Biomed. Res* 1991; 18: 333–345.
5. Burkard ME, Van Liew HD. Simulation of exchanges of multiple gases in bubbles in the body. *Respir. Physiol* 1994.
6. Srinivasan RS, Gerth WA, Powell MR. Increasing activity of h2-metabolizing microbes lowers decompression sickness risk in pigs during h2 dives. *J. Appl. Physiol.* 1999; 86: 732–741.
7. McDonough PM and Hemmingsen EA. Bubble formation in crabs induced by limb motions after decompression. *J. Appl. Physiol.: Respirat. Environ. Exercise Physiol.* 1984; 57: 117–122.
8. Hyldegaard O, Madsen J. Influence of heliox, oxygen, and n20-o2 breathing on n2 bubbles in adipose tissue. *Undersea Biomed. Res.* 1989; 16: 185–193.
9. Hyldegaard O, Madsen J. Effect of air, heliox, and oxygen breathing on air bubbles in aqueous tissues in the rat. *Undersea Hyperb Med* 1994; 21: 413–423.
10. Newhouse VL, Shankar PM. Bubble size measurements using nonlinear mixing of two frequencies. *J. Acoust. Soc. Am.* 1984; 75: 1473–1477.
11. Leighton TG, Lingard RJ, Walton AJ, Field JE. Acoustic bubble sizing by combination of subharmonic emissions with imaging frequency. *Ultrasonics* 1991; 29: 319–323.
12. Dunford RG, Vann RD, Gerth WA, Pieper CF, Huggins K, Wacholtz C, Bennett PB. The incidence of venous gas emboli in recreational diving. *Undersea Hyperb Med* 2000; 27.
13. Brubakk AO, Eftedal O. Comparison of three different ultrasonic methods for quantification of intravascular gas bubbles. *Undersea Hyperb Med* 2001; 28: 131– 136.
14. Neuman TS, Hall DA, Linaweaver PG. Gas phase separation during decompression in man: ultrasonic monitoring. *Undersea Biomed. Res.* 1976; 3: 121–130.
15. Watt DG, Lin YC. Doppler detection of thresholds for decompression-induced venous gas emboli in the awake rat. *Aviation Space & Environmental Medicine* 1979; 50: 571–574.
16. Minnaert M. On musical air-bubbles and sounds of running water. *Phil. Mag.* 1933; 16: 235–248.
17. Tiemann K, Pohl C, Schlosser T, et al. Stimulated acoustic emission: Pseudo-doppler shifts seen during the destruction of nonmoving microbubbles. *Ultrasound in Med. & Biol.* 2000; 26: 1161–1167.
18. Cathignol D, Chapelon JY, Newhouse VL, Shankar PM. Bubble sizing with high spatial resolution. *IEEE Trans. Ultrason. Ferr.* 1990; 37: 30–37.
19. Magari PJ, Kline-Shoder RJ, Stoedefalke BH, Butler BD. A non-invasive, *in vivo*, bubble sizing instrument. *IEEE Ultrasonics Symposium* 1997; 2: 1205–1210.
20. Buckey JC, Knaus DA, Alvarenga DL, Kenton MA, Magari PJ. Dual-frequency ultrasound for detecting and sizing bubbles. *Acta Astronautica* 2005; 56: 1041–1047.
21. Frinking PJA, de Jong N. Acoustic modeling of shell-encapsulated gas bubbles. *Ultrasound in Med. & Biol.* 1998: 24, 523–533.
22. Chappell MA and Payne SJ. A physiological model of the interaction between tissue bubbles and the formation of blood-borne bubbles under decompression. *Phys. Med. Biol.* 2006; 51: 2321–2338.
23. Morse PM, Ingard KU. Theoretical Acoustics. McGraw-Hill Book Company, 1968.
24. Bushberg TJ, Siebert JA, Leidholdt EM, Boone JM. The Essential Physics of Medical Imaging, 2nd edition, Lippincott Williams & Wilkins, 2002.